Desalination and Water Treatment
www.deswater.com
doi: 10.1080/19443994.2015.1004115

57 (2016) 5858–5878
March

Taylor & Francis
Taylor & Francis Group

Adsorption of methylene blue dye from aqueous solution by novel biomass *Eucalyptus sheathiana* bark: equilibrium, kinetics, thermodynamics and mechanism

Sharmeen Afroze[a,*], Tushar Kanti Sen[a], Ming Ang[a], Hiroshi Nishioka[b]

[a]*Department of Chemical Engineering, Curtin University, GPO Box U1987, Perth, Western Australia 6845, Australia, Tel. +61 8 9266 4045; Fax: +61 8 9266 2681; emails: sharmeen.afroze@postgrad.curtin.edu.au (S. Afroze), T.Sen@curtin.edu.au (T.K. Sen), M.Ang@curitn.edu.au (M. Ang)*

[b]*Graduate School of Engineering, University of Hyogo, 2167 Shosha, Himeji-shi, Hyogo 671-2280, Japan, email: ugh91055@nifty.com (H. Nishioka)*

Received 10 June 2014; Accepted 27 December 2014

ABSTRACT

This study was undertaken to evaluate the adsorption potential of a naturally available, cost-effective, raw eucalyptus bark (EB) (*Eucalyptus sheathiana*) biomass, to remove organic methylene blue (MB) dye from its aqueous solutions. Effects of various process parameters such as initial dye concentration, adsorbent loading, solution pH, temperature, presence of salts, mixture of dyes and surfactant onto MB dye adsorption by bark material were studied. Significant effect on adsorption was witnessed on varying the pH of the MB solutions. Results showed that the optimum pH lies between 7.4 and 10.0. The extent (%) of MB adsorption from aqueous solution decreased with the increase in the initial MB dye concentration, but increased with rise in temperature. The extent of MB dye adsorption was found to be enhanced due to increase of salts concentration. This is because of salting-out-effect, which comprises the changes of various short range forces. The overall kinetic studies showed that the MB dye adsorption by EB biomass followed pseudo-second-order kinetics. The mechanism of MB dye adsorption was analysed by intra-particle diffusion model and desorption study. Free energy change of adsorption (ΔG°), enthalpy change (ΔH°) and entropy change (ΔS°) were calculated to predict the nature of adsorption. The Langmuir adsorption isotherm model yields a better correlation coefficient than the Freundlich model and the dimensionless separation factor "R_L" indicated favourable adsorption process. The maximum Langmuir monolayer adsorption capacity of raw EB for MB dye was found to be 204.08 mg/g at 30°C. A single-stage batch adsorber design for MB dye adsorption onto EB biomass has been presented based on the Langmuir isotherm model equation. The results obtained in this study suggest a promising future for inexpensive raw EB biomass as a novel adsorbent and a better alternative to activated carbon adsorbent used for the removal of MB dye from dye bearing effluents.

Keywords: Eucalyptus bark biomass; MB adsorption; Desorption; Kinetic model; Isotherm

*Corresponding author.

1. Introduction

Excessive release of inorganic/organic pollutants into water due to industrialization, agricultural operations and urbanization has posed a great environmental problem worldwide. Many industries such as textile, leather, paper, plastics, tannery, cosmetics, rubber and paint use dyes to colour their products, which are some of the sources that generate dye bearing effluents [1]. The discharge of dyes into the environment is a concern for both toxicological and aesthetical reasons as dyes impede light penetration, damage the quality of the receiving streams, toxic to food chain organisms [2] and sometimes even carcinogenic [3,4]. Furthermore, the dyes have a tendency to sequester metal and may cause micro-toxicity to fish and other organisms [5].

Methylene blue (MB) is a cationic dye which is most commonly used for colouring and also used in microbiology, surgery, diagnostics [6,7]. Though MB is not strongly hazardous, it can cause some harmful effects. Acute exposure to MB can cause increased heart rate, shock, Heinz body formation, cyanosis, jaundice, quadriplegia and tissue necrosis in humans [8]. MB causes eye burns, which may be responsible for permanent injury to the eyes of human and animals [9]. Hence, the treatment of effluents containing such dye is of interest due to its harmful impacts on receiving waters. In general, dyes are poorly biodegradable or resistant to environmental conditions and therefore create the major problem in the treatment of wastewater containing dyes [9]. A range of technologies such as coagulation, foam flotation, precipitation, ozonation, ion exchange, filtration, solvent extraction, electrolysis, chemical oxidation, membrane technology, liquid–liquid extraction and adsorption on activated carbon have been used for the removal of dye contaminants from wastewater [10]. Among these methods, adsorption has been found to be an efficient and economic process to remove dyes, pigments and other colourants and to control the biochemical oxygen demand [11]. Commercial activated carbon has been successfully used in the removal of inorganics/organics from their aqueous phase. However, utilization of commercial activated carbon possesses limitation because of their high-cost and regeneration problem. Therefore, the current research is focused in finding a more cost-effective and efficient adsorbent in comparison with activated carbon [12–14]. The use of agricultural solid wastes as adsorbents for wastewater treatment has been identified because of their good adsorption potential due to the presence of carboxyl, hydroxyl and amino groups over their surfaces [15]. Therefore, a number of non-conventional cost-effective adsorbents such as cashew nut shell [16], raw and modified pine cone [12], pine leaves [17], pine cone biomass [9], wood apple shell [18], rice husk [8], orange peels [19], banana peel [19] and caster seed shell [20] have been used for the removal of MB dye from its aqueous solution. Readers are encouraged to go through various recently published review article by Yagub et al. [21], Salleh et al. [13] and Ali et al. [22] towards dye removal by various adsorbents. On the utilization of agricultural solid waste as an effective adsorbent, their easy availability, low-cost and good adsorption potential make the adsorption process more attractive [23].

Eucalyptus trees (*Eucalyptus sheathiana*), which are evergreen and one type of lignocellulose carbonaceous material, form about three-quarters of the tree flora of Australia. They are fast growing and abundantly available worldwide. Due to the high number of eucalyptus trees in Australia, massive amounts of barks (as waste) are disposed each year. Eucalyptus bark (EB) was used as a sorbent for the removal of reactive dyes for cellulose fibres (Remazol BB) [24], Cd(II) ions [25], chromium ions [26], Cu(II), Cr(III), Cd(II) and Ni (II) [27], mercury(II) [28], eriochrome black T [29], MB dye [30] from aqueous solutions. Basically, there are only few reported works on the application of EB biomass as an effective adsorbent and mostly limited towards inorganic removal. Therefore, this research work was undertaken to explore the potential use of raw EB biomass as a cost-effective and efficient adsorbent in the removal of MB dye from its aqueous solution at various physico-chemical conditions. Further, large amount of salts and surfactant is utilized in the dyeing process, and there should be an effect of dissolved and mixed salt concentration and surfactant combination on the adsorption capacity of biomass. Therefore, mixed salt effect and surfactant effect on MB dye adsorption which is further new aspect of this study have also been presented here. The adsorption characteristics vary quantitatively and qualitatively with the nature of agricultural biomass, its processing and its origin [12,17]. Hence, it is necessary to understand the kinetics and mechanism of adsorption under various process conditions, which will help the selection of designing of an adsorption column and adsorbent system. Despite the fact that the industrial effluents contain several pollutants simultaneously, therefore the effect of mixed dyes on MB dye adsorption has also been studied here which is another new aspect of this research area. The effect of operating conditions such as solution pH, sorbent dosage, initial MB dye concentration, temperature, contact time, presence of salts, mixture of dyes and addition of surfactant and their optimum values was investigated on the adsorption efficiency of MB dye. The adsorption

equilibrium data were analysed using Langmuir and Freundlich models. In addition, thermodynamic parameters were determined for the sorption of MB dye to explain the process feasibility, and desorption efficiency was also calculated to investigate the mechanism and recovery of MB dye together with the regeneration and reusable capacity of the biosorbent. In order to gain insight into the dynamics of the process, a single-stage batch adsorber has been designed for the removal of MB dye by EB based on the equilibrium data obtained.

2. Materials and methods

2.1. Adsorbent

E. sheathiana (family name: Myrtaceae) barks were obtained from Curtin University—Bentley Campus, Western Australia, and it was collected between February and March 2013. The barks were washed repeatedly with distilled water to remove impurities such as sand and leaves and then dried at 105˚C for 24 h in an oven. The dried biomass was ground using a mechanical grinder by RETSCH, GmbH & Co. KG, West Germany, to fine powder and passed through British Standard Sieves (BSS) of 106 μm. The powder EB biomass was then stored in an airtight plastic container and was used for analysis as well as for conducting adsorption experiments. The biomass sample was characterized in terms of surface area, bulk density and percentage of elemental analysis (nitrogen, carbon and hydrogen) was done by 2400 Series II CHNS/O analyser by Perkin Elmer. Bulk density of raw EB was measured as per the below equation: [31].

$$\text{Bulk Density} = \frac{\text{Mass of dry sample (g)}}{\text{Total volume used (ml)}} \quad (1)$$

Further, EB biomass powder was analysed by the Spectrum 100 FTIR spectrometer to determine functional groups. Scanning electron microscope (SEM) (EVO 40) and transmission electron microscope (TEM) were used for the information of the surface morphological structure of EB before and after adsorption. Particle size of EB powder was measured by Malvern Hydro 2000S master Sizer, Malvern Instruments Ltd, UK. Brunauer–Emmett–Teller (BET) method was used to determine BET surface area using Tristar II 3020, Micromeritics Instrument Corporation.

2.2. Adsorbate and other chemicals

All chemicals used were of analytical grade. MB, the typical basic cationic dye, was selected as the adsorbate in this study. The formula of MB dye is $C_{16}H_{18}N_3SCl.3H_2O$ with a molecular weight of 319.86 g/mol was supplied by Sigma–Aldrich Pty. Ltd, NSW, Australia. A stock solution of 1,000 ppm MB was prepared by dissolving the appropriate amount (1,000 mg) of MB in a litre of ultra-pure water. The working solutions were prepared by diluting the stock solution with ultra-pure water to give the appropriate concentration of the working solutions. Similarly, solutions of 100, 200 and 300 ppm were prepared by dissolving the appropriate amount of laboratory grade NaCl, $CaCl_2$ and $FeCl_3$ separately in a litre of ultra-pure water to perform experiments with salt effects. Triton X-100 (average mol. wt. 625, purity ≤100%) was used as nonionic surfactant and was procured from Sigma–Aldrich Pty. Ltd, NSW, Australia. The pH of the solutions was adjusted by addition of either 0.1 M HCl or 0.1 M NaOH solutions, respectively. All sample bottles and glassware were cleaned and then rinsed with deionized water and oven-dried at 60˚C.

The SP-8001 UV/VIS spectrophotometer was used to determine the concentrations of MB dye in solution. pH measurements were taken using WP-81 pH-Cond-Salinity meter. The concentration of the residual dye was measured using UV/visible spectrometer at a λ_{max} corresponding to the maximum adsorption for the dye solution (λ_{max} = 665 nm) by withdrawing samples at fixed time intervals and centrifuged, and the supernatant was analysed for residual MB. Calibration curve was plotted between absorbance and concentration of the dye solution to obtain absorbance–concentration profile.

2.3. Adsorption experiments

2.3.1. Kinetic experiments

Batch adsorption experiments were conducted by varying the initial solution pH, adsorbent dose, initial dye concentration, salts, mixed dye concentrations, surfactant and temperature at predetermined time intervals. These adsorption batch experiments were conducted as per our earlier published method [9]. The mixture was shaken in a constant temperature Thermo Line Scientific Orbital Shaker Incubator at a speed of 120 rpm and temperature of 30˚C. At predetermined time, the bottles were withdrawn from the shaker and the residual dye solution was separated from the mixture by centrifuging. The absorbance of the supernatant was measured at the wavelength that corresponds to the maximum absorbance of the sample, and the dye concentration was calculated from the linear equation of the calibration curve. The

amount of dye adsorbed onto EB biomass at time t, q_t (milligrams per gram) and % adsorption are calculated from Eqs. (2) and (3), respectively:

$$q_t = \frac{(C_0 - C_t)V}{m} \tag{2}$$

and dye removal efficiency, that is % of adsorption, was calculated as:

$$\%\,\text{adsorption} = \frac{C_0 - C_t}{C_0} \times 100 \tag{3}$$

where C_0 is the initial dye concentration (milligrams per litre), C_t is the concentration of dye at any time t (min), V is the volume of dye solution (l), and m is the mass of EB powder (g). All experimental measurements are within ±10% accuracy.

2.3.2. Isotherm experiments

Equilibrium adsorption studies were conducted by contacting 50 ml of dye solutions of different initial concentration of 20, 30, 40, 50, 60 and 70 ppm with 20 mg of EB powder in a series of 250-ml conical flasks for a period of 3 h which was more than sufficient to achieve equilibrium time. The method was also as per our earlier published method [9].

2.4. Theory

2.4.1. Adsorption kinetics and mechanism

In order to investigate the mechanism of adsorption and the transient behaviour of the dye adsorption process, adsorption kinetics were evaluated and analysed using pseudo-first-order, pseudo-second-order and intra-particle diffusion models as explained below.

2.4.1.1. Pseudo-first-order and pseudo-second-order kinetic models. Pseudo-first-order model was developed by Lagergren [32]. The linearized integral form of the pseudo-first-order is generally expressed as [33]:

$$\log(q_e - q_t) = \log(q_e) - \frac{K_1}{2.303}t \tag{4}$$

where q_e and q_t refer to the amount of MB adsorbed (mg/g) at equilibrium and at time, t (min), respectively. K_1 is the equilibrium rate constant of pseudo-first-order adsorption (min^{-1}). A plot of log $(q_e - q_t)$ vs. time, t, gives the value of K_1, and q_e can be calculated.

Similarly, the linearized form of the pseudo-second-order kinetic model [34] is shown in below equation:

$$\frac{t}{q_t} = \frac{1}{K_2 q_e^2} + \frac{1}{q_e}t \tag{5}$$

where K_2 is the equilibrium rate constant of pseudo-second-order adsorption [g/(mg min)]. A plot between t/q_t vs. t gives the value of rate constant K_2 (g/mg min), initial sorption rate h (mg/g-min), and also q_e (mg/g) can be calculated.

The constant K_2 is used to calculate the initial sorption rate h, at $t \to 0$, as follows:

$$h = K_2 q_e^2 \tag{6}$$

Thus, the rate constant K_2, initial adsorption rate h and predicted q_e can be calculated from the plot of t/q_t vs. time t using Eq. (5).

2.4.1.2. Intra-particles diffusion model. Intra-particle diffusion model is used for identifying the adsorption mechanism for design purpose [9]. For most adsorption processes, the amount of adsorption varies almost proportionately with $t^{0.5}$ rather than with the contact time [31].

$$q_t = K_{id}t^{0.5} + I \tag{7}$$

where q_t is the amount adsorbed at time t and $t^{0.5}$ is the square root of time. K_{id} is the rate constant for intra-particle diffusion (mg/g $\text{min}^{0.5}$) which can be calculated from the slope of the linear equation of the plot q_t against $t^{0.5}$. I (mg/g) is a constant that gives an idea about the thickness of the boundary layer.

2.4.2. Adsorption isotherm

To simulate the adsorption isotherm, two commonly used models, Freundlich [35] and Langmuir [36], were selected to explicate dye–EB interaction and to determine the capacity of adsorbent.

Freundlich Isotherm: The linearized Freundlich adsorption isotherm [35], which assumes that adsorption takes place on heterogeneous surfaces, can be expressed as:

$$\ln q_e = \ln K_f + (1/n)\ln C_e \tag{8}$$

where q_e (mg/g) is the equilibrium amount of dye adsorbed by the adsorbent, C_e (ppm) is the equilibrium concentration of adsorbate in solution, K_f and n are isotherm constants which indicate the capacity and the intensity of the adsorption, respectively [37].

Langmuir Isotherm: The Langmuir isotherm model [36] was developed to explain how adsorption takes place on homogeneous surfaces. The linearized forms of Langmuir types I and II can be written as per Eqs. (9) and (10), respectively.

$$\frac{C_e}{q_e} = \frac{1}{K_a q_m} + \frac{C_e}{q_m} \tag{9}$$

$$\frac{1}{q_e} = \left(\frac{1}{K_a q_m}\right)\frac{1}{C_e} + \frac{1}{q_m} \tag{10}$$

The maximum adsorption capacity q_m (mg/g) and Langmuir constant related to the energy of adsorption K_a (L/mg) were calculated from the slope and intercept of the linearized forms of the plots where (C_e/q_e vs. C_e) for Langmuir type I and ($1/q_e$ vs. $1/C_e$) for Langmuir type II, respectively. The separation factor (R_L) is dimensionless and is used to investigate the adsorption system feasibility at different initial dye concentrations [38], and it can be calculated from using following equation.

$$R_L = 1/(1 + K_a C_0) \tag{11}$$

where K_a is Langmuir constant and C_0 is the initial MB concentration (ppm). Favourable adsorption process takes place where R_L value is $0 < R_L < 1$ [39].

2.5. Thermodynamic study

Thermodynamic studies have been investigated based on the equilibrium data. The thermodynamic parameters, such as change in Gibbs free energy (ΔG°), enthalpy change (ΔH°) and change in entropy (ΔS°) for the adsorption of MB dye on EB adsorbent, have been determined using the following equations [31]:

$$\Delta G^\circ = \Delta H^\circ - T\Delta S^\circ \tag{12}$$

$$\log\left(\frac{q_e}{C_e}\right) = \frac{\Delta S^\circ}{2.303R} + \frac{-\Delta H^\circ}{2.303\mathrm{RT}} \tag{13}$$

where q_e is the solid-phase concentration at equilibrium (milligrams per litre), C_e is equilibrium concentration in solution (mg/L), T is temperature in K, and R is the gas constant (8.314 J/mol K). The entropy change (ΔS°) and enthalpy change (ΔH°) can be calculated from the intercept and slope of the linear Van't Hoff plot log (q_e/C_e) vs. $1/T$. From those values, Gibbs free energy (ΔG°) can be found using Eq. (12).

3. Results and discussion

3.1. Characterization of EB biomass adsorbent

Surface chemistry of EB such as specific surface area, pore volume distribution and pore size was measured, and physical characteristics of this biomass, such as bulk density, percentage of elemental analysis (nitrogen, carbon and hydrogen) were also done. All the results are presented in Table 1. Bulk density is important for commercial adsorption column design and also affects the performance of adsorption process. As per American Water Work association, bulk density should be greater than 0.25 g/cm^3 for practical purposes.

3.1.1. FTIR analysis

Fig. 1 shows the FTIR spectra of raw EB powder. Several peaks were observed from the spectra (Fig. 1), indicating that EB is composed of various functional groups which are responsible for binding of cationic dye MB. The absorption band at 3,000–2,850 cm^{-1} is presented with a peak band at about 2,920.6 and 2,851.6 cm^{-1} correspond to C–H stretching group [40]. Three peaks are found at 2,107.0, 2,140.6 and 2,148.3 cm^{-1} which can be described as weak −C≡C− alkyne bond [40]. The peaks at 2,251.1 and 2,284.6 cm^{-1} with C≡N stretches show nitrile functional group [41]. Peaks at 1,729.7, 1,619.3, 1,515.5, 1,445.7 and 1,370.3 cm^{-1} indicate strong ester group with C=O stretch [40], medium N–H bond with amine group [41], N=O stretch with nitro group [40], medium C–C bond in ring aromatics [41] and nitro group with N=O bond [40], respectively. The presence

Table 1
Physico-chemical properties of raw EB adsorbent

Parameters	Values
BET surface area (m^2/g)	6.55
Bulk density (gm/cm^{-3})	0.39
Pore volume (cm^3/g)	0.003432
Average pore size (A°)	18.42
Nitrogen, N (%)	0.24
Carbon, C (%)	42.32
Hydrogen, H (%)	5.69

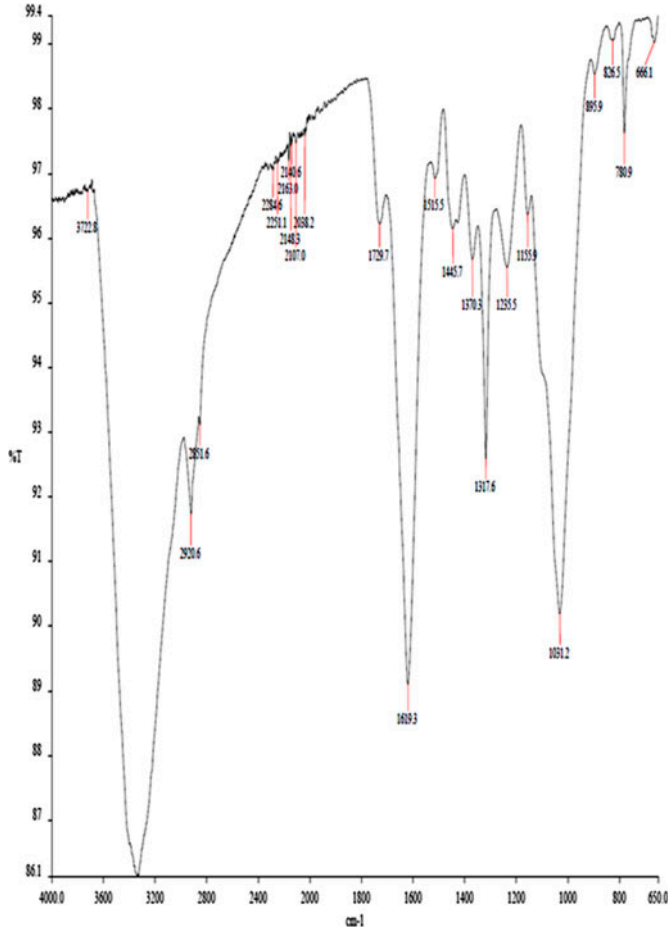

Fig. 1. FTIR spectrum of raw EB biomass (106 μm).

of alcohols, carboxylic acids, esters and ethers functional groups was observed through C–O strong stretch in the absorption band at 1,320–1,000 cm^{-1} frequency with absorption peaks at 1,317.6, 1,235.5, 1,155.9 and 1,031.2 cm^{-1} [40]. Alkene small =C–H absorption bend is found strongly in between 1,000 and 650 cm^{-1} having peaks at 895.9, 826.5, 780.9 and 666.1 cm^{-1} [40].

3.1.2. Spectrometric surface morphological analysis

Scanning electron micrograph (SEM) of EB biomass before and after adsorption is shown in Fig. 2(a) and (b), respectively. It is clear from the SEM pictures that EB is amorphous carbon with non-crystalline structures. The availability of pores and internal surface is clearly displayed in the SEM picture of the EB biomass before adsorption (Fig. 2(a)), and the coverage of the surface and the pores by the adsorbed MB is shown in Fig. 2(b). Basically, the porous structure that appears in Fig. 2(a) gets blurred in Fig. 2(b) because of adsorption.

Similar to SEM, TEM was also used to study and determine the particle shape and porous structure of biomass. The greater the number of pores, the greater will be the biosorption of dye onto the biosorbent surface. Typical TEM photographs of raw EB and MB loaded biomass are shown in Fig. 3(a) and (b). These photographs indicate the porous and fibrous texture of the biosorbent with high heterogeneity that could contribute to the biosorption of the dyes.

3.1.3. Particle size distribution

The particle size distribution of raw EB biomass was determined by Malvern Hydro 2000S master Sizer, Malvern Instruments Ltd., UK. The surface weighted mean particle size for EB adsorbent was found to be 25.26 μm while the specific surface area was 0.238 m^2/g.

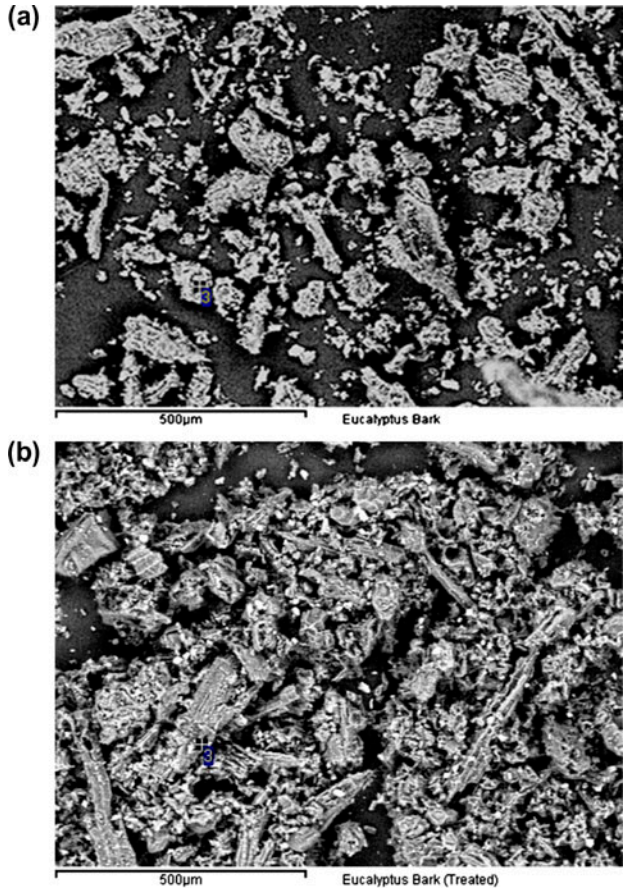

Fig. 2. (a) SEM images of raw EB biomass before adsorption. (b) SEM images of same raw EB biomass after MB adsorption.

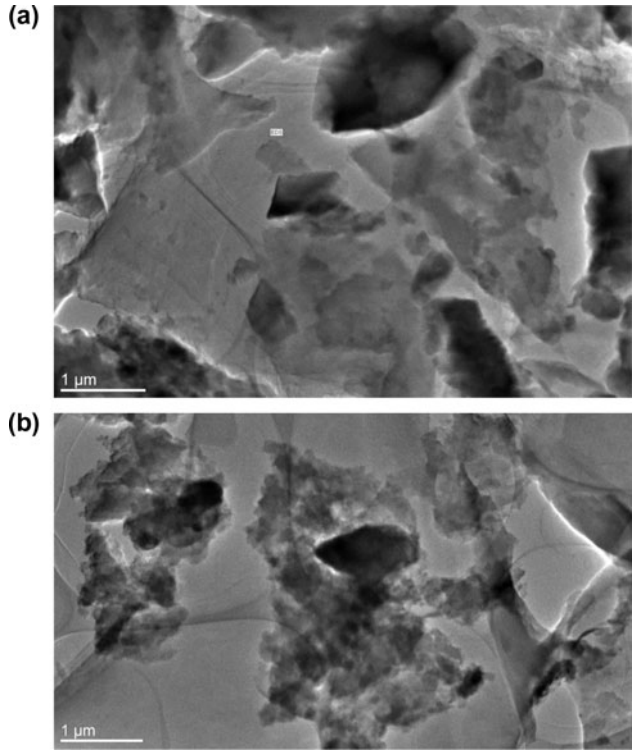

Fig. 3. (a) TEM images of raw EB biomass before adsorption. (b) TEM images of same EB biomass after MB adsorption.

3.1.4. BET analysis

The specific surface area was calculated by the BET equation, while the total pore volume (V_T) was evaluated by converting the adsorption volume of nitrogen at relative pressure 0.95 to equivalent liquid volume of the adsorbate [42]. Prior to analysis, the sample was degassed to eliminate any trace of volatile elements at room temperature for 1 h then increasing the temperature to 120˚C for 6 h. The sample was then transferred to the analysis system where it was cooled in liquid nitrogen. The calculated BET surface area, pore volume and pore radius of the EB biomass are presented in Table 1.

3.2. Adsorption kinetic experiments

3.2.1. Effect of initial solution pH on MB dye adsorption

The efficiency of adsorption depends on the solution pH because variation in pH leads to the variation in the degree of ionization of the adsorptive molecule and the surface properties of adsorbent [9]. Fig. 4 shows the effect of initial solution pH on amount of MB dye adsorption, q_t (milligrams per gram) and percentage removal of dye with solution pH. The amount of dye adsorption increases with time as well as with the increase in pH or alkalinity. The percentage removal of dye was also found to increase when the solution pH was increased from pH 2.5 to pH 10.0. From Fig. 4, it was found that the amount of dye adsorbed increased from 28.89 mg/g (57.80% removal efficiency) to 44.73 mg/g (89.45% removal efficiency) due to change in pH from 2.5 to 10.0 for a fixed initial dye concentration of 20 ppm at equilibrium. The observed pH trend clearly indicates that the maximum adsorption of MB dye takes place at pH 10.0. With the increasing pH values, the adsorption of MB on EB biomass tends to increase, which can be explained by the electrostatic interaction of cationic dye MB with the negatively charged surface of the EB. This electrostatic force of attraction is more with increasing negative surface charge of adsorbent. This was supported by point of zero surface charge, pH_{zpc} of EB of 2.2 [29]. Further, the high percentage of dye removal at high pH is also due to the presence of less H^+ competing

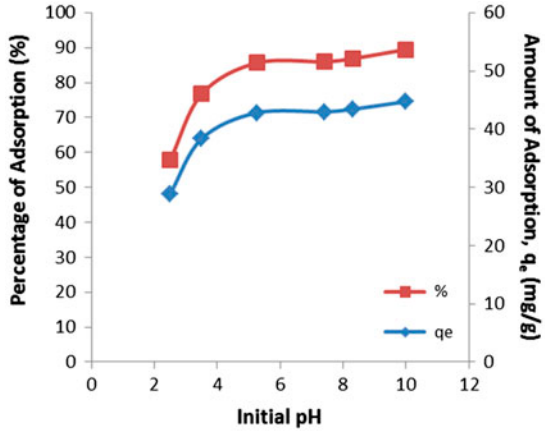

Fig. 4. Effect of initial solution pH on the adsorption of MB dye onto EB powder: (conditions: mass of adsorbent = 20 mg, volume of MB solution = 50 ml, initial MB dye concentration = 20 ppm, temp = 30˚C, shaker speed = 120 rpm and time of adsorption = 180 min).

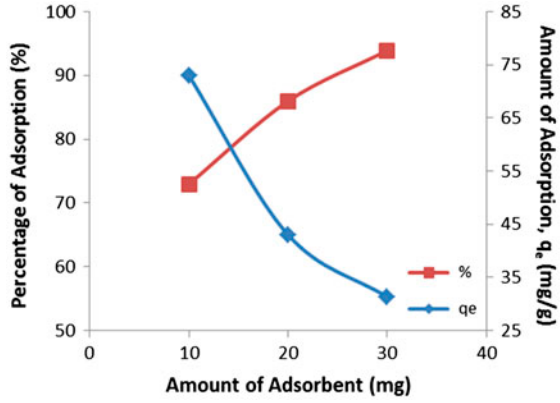

Fig. 5. Effect of adsorbent dosages on the adsorption of MB dye onto EB powder: (conditions: volume of MB solution = 50 ml, solution pH 7.4, initial MB dye concentration = 20 ppm, temp = 30˚C, shaker speed = 120 rpm and time of adsorption = 180 min).

for sorption sites on the biomass. Low pH leads to an increase in H^+ ion concentration in the system, and the surface of bark biomass acquires positive charge by protonation of phenolic and amino groups of EB surface [29], and hence, less amount of cationic MB dye adsorption takes place. The pH of the final MB dye solution is the result of electrostatic interaction between negatively charged EB adsorbent surface and cationic MB dye solution to form complex, and more H^+ ions came into solution which gives little decrease of the final solution pH [9].

Similar trend was reported for adsorption of MB onto rice husk [8], palm kernel shell activated carbon [43] and wheat shells [44].

3.2.2. Effect of adsorbent dosage on MB dye adsorption

To investigate the effect of adsorbent EB dose for the adsorption of MB dye, the experiments were conducted with different adsorbent doses (0.01–0.03 g/50 ml) while maintaining the initial dye concentration (20 ppm), temperature (30˚C), pH (7.4) and shaker speed (120 rpm) constant at different contact times. Fig. 5 shows that at equilibrium, the percentage dye removal was increased from 72.95 to 94% with the increase of adsorbent mass from 0.01 to 0.03 g. It was also found that the increase in adsorbent dosage from 0.01 to 0.03 g resulted in decrease of amount of adsorbed dye from 72.96 to 31.30 mg/g (Fig. 5).

At higher EB to MB concentration ratios, there is a very fast superficial sorption onto the EB surface that gives a lower MB concentration in the solution compared to the lower biomass to MB concentration ratio. This is because a fixed mass of EB can only adsorb a fixed amount of dye. Therefore, the higher the adsorbent dosage, the larger the volume of effluent that a fixed mass of EB biomass can purify. The decrease in amount of dye adsorbed, q_e (mg/g) with increasing adsorbent mass, is due to the split in the flux or the concentration gradient between solute concentration in the solution and the solute concentration in the surface of the adsorbent [9,31]. Thus, with increasing adsorbent mass, the amount of dye adsorbed onto unit weight of adsorbent gets reduced and hence causing a decrease in q_e value with increasing adsorbent mass concentration [8]. A similar behaviour was observed for mercury (II) removal on EB [28] and MB adsorption on guava leaf [45], on gulmohar plant leaf [46] and on cashew nut shell activated carbon [47]. Further increasing the amount of the adsorbent and keeping adsorbate concentration fixed make a large number of sites available for a fixed concentration of adsorbate, hence the increase in percentage (%) of adsorption and decrease in the value of q_e [20].

3.2.3. Effect of initial dye concentration and contact time on MB adsorption kinetics

The effect of contact time on the adsorption of MB dye was investigated at different initial dye concentration onto EB adsorbent, and results are presented in Fig. 6(a) and (b), respectively. From Fig. 6(a), it is observed that the amount of MB dye adsorption, q_t (milligrams per gram), increased from 43 to 67.91 mg/g with increase in initial MB dye concentration from 20 to

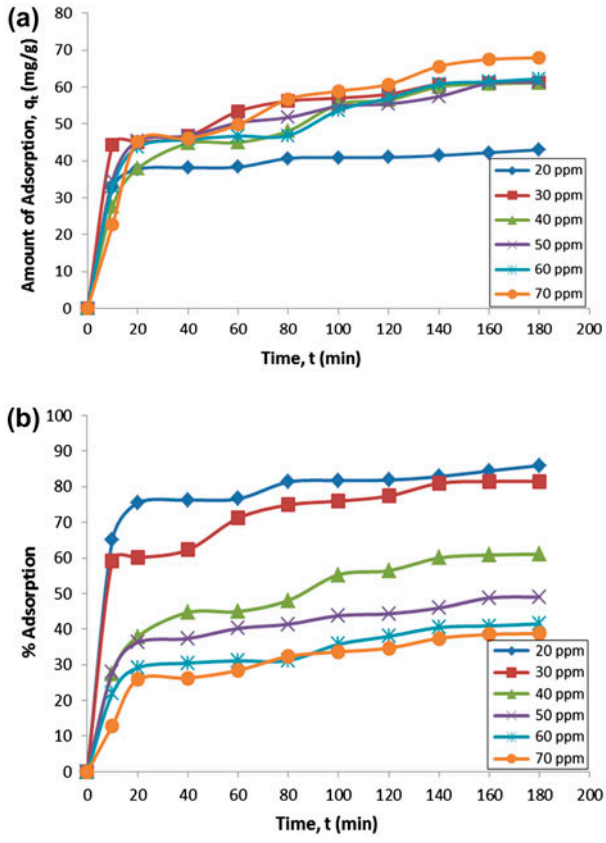

Fig. 6. (a) Effect of initial solution concentration on the adsorption of MB dye onto EB powder: (Conditions: mass of adsorbent = 20 mg, volume of MB solution = 50 ml, Solution pH 7.4, temp = 30˚C and shaker speed = 120 rpm). (b) Effect of initial solution concentration on the extent (%) of adsorption of MB dye onto EB powder: (conditions: mass of adsorbent = 20 mg, volume of MB solution = 50 ml, solution pH 7.4, temp = 30˚C and shaker speed = 120 rpm).

70 ppm. Further, it was found that the amount of adsorption, that is milligrams of adsorbate per gram of adsorbent, increases with increasing contact time at all initial dye concentrations and equilibrium is attained within 140 min. It was also found from Fig. 6(b) that the percentage removal of dye increased from 38.81 to 85.95% with decreasing initial concentration of MB dye from 70 to 20 ppm. Basically, from both Fig. 6(a) and (b), the adsorption percentage decreases and the amount of adsorption increases with increasing initial dye concentration. This is because of the initial dye concentration provides the driving force to overcome the resistance to the mass transfer of dye between the aqueous and the solid phase. For constant dosage of adsorbent, at higher initial dye concentration, the available adsorption sites of adsorbent become fewer, and hence, the removal of MB depends upon the initial concentration [48]. The increase in initial dye concentration also enhances the interaction between adsorbent and dye. Therefore, an increase in initial dye concentration leads to increase in the adsorption of dye. It is also found from Fig. 6(b) that the removal of dye by adsorption on EB was very fast at the initial period of contact time but slowed down with time. These kinetic experiments [Fig. 6(a) and (b)] clearly indicated that adsorption of MB dye on EB is a more or less two-step process: a very rapid adsorption of dye to the external surface followed by possible slow intra-particle diffusion in the interior of the adsorbent. The rapid kinetics has significant practical importance, as it facilitates smaller reactor volumes, ensuring high efficiency and economy [38].

Similar type of results was reported by various researchers for MB adsorption on oak sawdust [49], on acid activated carbon [50], on pine cone [9] and on activated carbon prepared from rice husk [51].

3.2.4. Effect of temperature on MB dye adsorption

Real textile effluents are mostly released at relatively higher temperatures, so temperature is also an important design parameter for the real application of biosorption process [23]. There are two major effects of temperature on the adsorption process: increasing the temperature is known to increase the rate of diffusion of the adsorbate molecules across the external boundary layer and in the internal pores of the adsorbent particle, owing to the decrease in the viscosity of the solution [52]. In addition, changing the temperature will change the equilibrium capacity of the adsorbent for a particular adsorbate [52].

Fig. 7 depicts the effects of solution temperature on the adsorption of MB dye onto EB adsorbent where it has been revealed that the amount of adsorption, q_t (mg/g), increased with increase in temperature. It was also found that the increase in temperature from 30 to 60˚C resulted in increase in the extent of (%) adsorption from 85.97 to 90.79% for which plot is not presented here. The fact that the adsorption of dye was in favour of temperature indicates that the mobility of the dye molecule increased with increase in temperature. This implies that the dye molecule should interact more effectively with the adsorbent surface with rise in temperature. The increase in adsorption capacity with increasing temperature suggests that the process of removal of MB dye by EB biomass is endothermic in nature. Similar types of results were reported by other researchers for MB adsorption on water weeds biomass [53], cashew nut shell [16] and NaOH-modified malted sorghum mash [54].

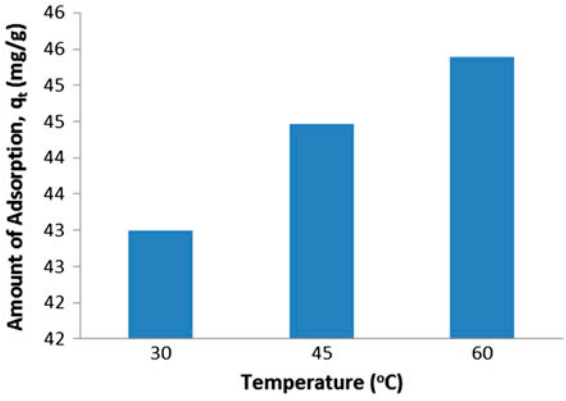

Fig. 7. Effect of temperature on the adsorption of MB dye onto EB powder: (conditions: mass of adsorbent = 20 mg, volume of MB solution = 50 ml, solution pH 7.4, initial MB dye concentration = 20 ppm, shaker speed = 120 rpm and time of adsorption = 180 min).

3.2.5. Effect of presence of salts on MB dye adsorption kinetics

In general, textile industries consume large amount of salts during the dyeing process, and hence, the effect of salts on adsorption has to be evaluated. The presence of these salts in textile effluents is one of the important factors that control both electrostatic and non-electrostatic interactions between the biosorbent surface and dye molecules and therefore affects the biosorption capacity [23,55]. To examine how salt concentration affects adsorption of MB onto EB biomass explored in this paper, we added NaCl, $CaCl_2$ and $FeCl_3$ of concentrations ranging from 100 to 300 ppm to the MB solution. The results are presented in Fig. 8. The effect of salts on MB dye adsorption was conducted at a solution pH of 7.4 where dyes and adsorbent EB were oppositely charged. It was found from Fig. 8 that the MB dye removal capacity by EB was decreased due to the presence of monovalent NaCl salt and it was more significantly decreased with decreasing salt concentration. Similar trend was observed for divalent $CaCl_2$ salt but comparatively to a lesser extent. This was due to the attractive electrostatic forces between the adsorbent surface and adsorbate ions, whereas for trivalent salt system, electrostatic attraction was repulsive and hence an increase in ionic strength also increased adsorption (Fig. 8) [56–58]. Bharathi and Ramesh [56] also reported that the electrical double layer surrounding the adsorbent surface was compressed due to the presence of increasing salt concentration which may lead to a decrease in the electrostatic potential and hence a reduction of coulombic free energy and a decrease in basic dye adsorption as in the case of NaCl-MB and $CaCl_2$-MB system. Further Fig. 8 indicates that the adsorption of positively charged MB on negatively charged EB biomass (at this pH) enhanced with the nature of salt in the order of $Na^+ < Ca^{++} < Fe^{+++}$. Wang et al. [59] reported that the amount of adsorption depends on the nature of electrolytes such as chloride salt of sodium which favours attractive electrostatic forces. The percentage of MB removal was increased with the increase in trivalent $FeCl_3$ salt concentration when compared with the results of MB adsorption without salt. For $FeCl_3$-MB system, this behaviour may be due to the dye

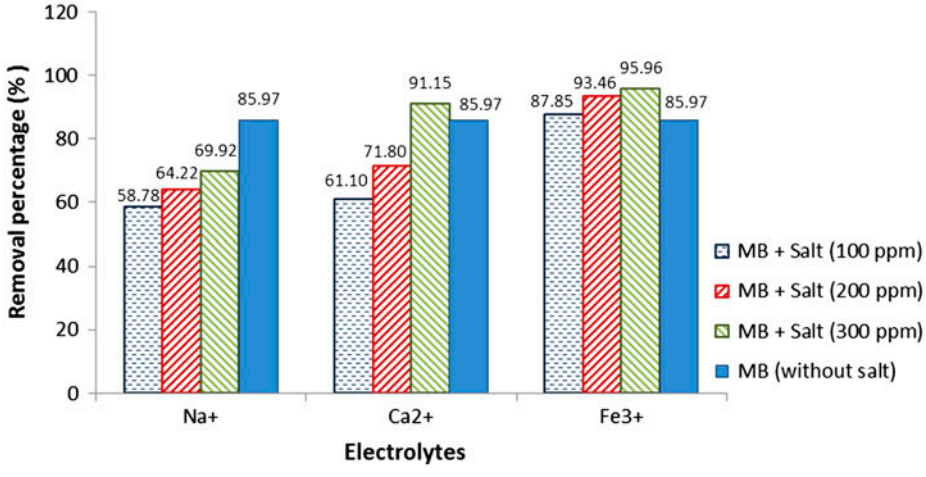

Fig. 8. Effect of electrolytes on the extent (%) of adsorption of MB dye onto EB powder: (conditions: mass of adsorbent = 20 mg, total reaction volume = 50 ml (48 ml of MB solution + 2 ml salt solution), initial MB dye concentration = 20 ppm, solution pH 7.4, temp = 30˚C, shaker speed = 120 rpm and time of adsorption = 180 min).

dimerization in solution or formation of dye aggregation induced by the effect of salt ions which is known as "salting-out-effect" [57,58]. Basically, various types of short range forces such as Van der Waals force, dipole–dipole and ion–dipole force increased with salt concentration during dye dimerization [58]. From Fig. 8, it is also observed that the amount of MB adsorption significantly increased with divalent/trivalent salt cations compared to monovalent cations. This may be due to increase in surface charge density of Ca^{2+}/Fe^{3+} compared to Na^{+} ions at this medium solution pH range where precipitation was nil.

Further in Fig. 9, it is also observed that by mixing monovalent (Na^{+}) and divalent (Ca^{2+}) electrolytes, at equilibrium, the amount of adsorption (q_t) became much higher (54.69 mg/g) compared to the electrolytes added separately to the solution (29.39 mg/g for NaCl and 30.55 mg/g for $CaCl_2$). It is known that the presence of salt formed by strong acid and alkali increases the ionic strength of the solution. This increase in ionic strength boosts the adsorption based on electrostatic interactions and thus increases adsorption capacities of MB dye as shown in Fig. 9. Therefore, increase in ionic strength was found to have an increase in adsorption of MB dye onto EB biomass.

3.2.6. Removal of mixed cationic dye (MB) and anionic dye (CR) simultaneously by raw EB biomass

In this group of experiments, mixed adsorption of MB and Congo red (CR) dye from their binary solutions was investigated by following a similar procedure as described in earlier section. These studies were performed at an initial pH of 7.4 and at a temperature of 30˚C.

From Fig. 10, it is found that the percentage removal of MB was higher (86.33%) compared to CR removal (57.95%) at a particular solution pH of 7.4. At this solution pH of 7.4, the surface charge is mostly negative in nature and hence large amount of cationic dye MB adsorption due to electrostatic force of attraction compared to less amount of anionic dye CR adsorption. However, EB material can be used to remove both cationic and anionic dye from its aqueous solution. CR dye removal was higher at acidic solution for which plot is not presented here.

3.2.7. Effect of surfactant on MB dye adsorption

Surfactants are used in the textile industries during different washing processes [60]. Surfactant Triton X-100 was added (1%) to the 50 ml of 20 ppm MB dye solution to check out the effect of surfactant on the MB dye removal from the solution which is presented in Fig. 11. From Fig. 11, it is clearly seen that the percentage of MB dye removal in the absence of surfactant was 85.97%, whereas the percentage of MB dye removal in the presence of non-ionic surfactant Triton X-100 decreased to 76.08%. This might be due to the competition between dye molecules and surfactants for the attachment to the biosorbent surface [23,61]. Decrease in MB dye removal in the presence of non-ionic surfactant was also observed by [62]. Similar trend of decrease in biosorption capacity of biosorbent

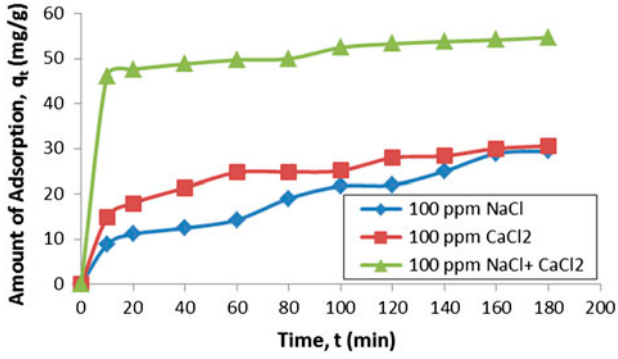

Fig. 9. Effect of mixture of electrolytes on the adsorption of MB dye onto EB powder: (conditions: mass of adsorbent = 20 mg, total reaction volume = 50 ml (48 ml of MB solution + 2 ml salt solution), initial MB dye concentration = 20 ppm, solution pH 7.4, temp = 30˚C, shaker speed = 120 rpm).

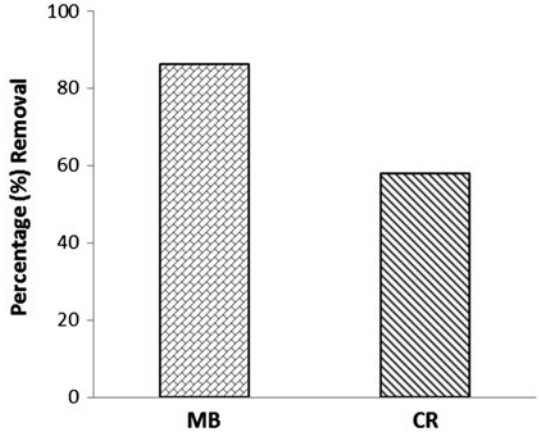

Fig. 10. Effect of mixture of adsorbents on the adsorption onto EB powder: (conditions: mass of adsorbent = 20 mg, volume of MB solution = 25 ml, volume of CR solution = 25 ml, initial MB concentration = 20 ppm, initial CR concentration = 20 ppm, temp = 30˚C, shaker speed = 120 rpm and time of adsorption = 180 min).

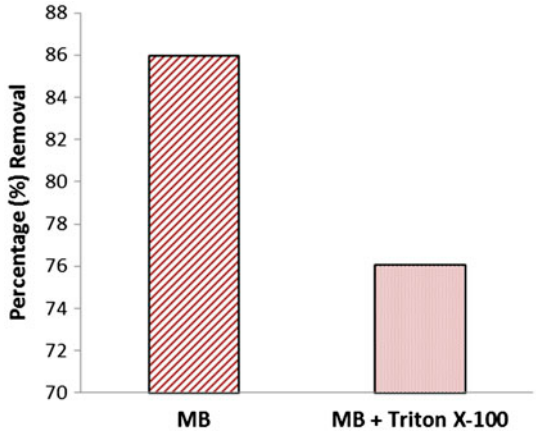

Fig. 11. Effect of surfactant on the extent (%) of adsorption of MB dye onto EB powder: (conditions: mass of adsorbent = 20 mg, volume of MB solution = 50 ml, initial MB dye concentration = 20 ppm, volume of Triton X-100 = 1.0 ml, temp = 30°C, shaker speed = 120 rpm and time of adsorption = 180 min).

in the presence of surfactants was further reported by Brahimi-Horn et al. [63] and by Sadaf and Bhatti [23].

3.3. Desorption studies

Desorption is important for various reasons such as for identification of adsorption mechanism, reusability of adsorbents, recovery of contaminants and reduction of secondary wastes. In desorption studies, the loaded raw EB adsorbent that was used for the adsorption of MB dye solution was separated from solution by centrifugation and then dried. The dried adsorbent was agitated with 50 ml of distilled water at different pH values (2.5–8.7) for the predetermined equilibrium time of the adsorption process, and the desorbed dye was then determined. It was found that per cent desorption decreased with increase in pH of the aqueous medium for which plot is not shown here. Desorption tests showed that maximum dye releasing of 46.18% was achieved in aqueous solution at pH 2.5 within these pH ranges (Table 2).

In acidic medium such as nitric acid (HNO_3), the protons in solution replace the MB ions on the biomass surface, while the apparent poor recovery of less than 10% observed in basic media such as NaOH may be due to the coordinating ligands being deprotonated; hence, bound-dye ions find it difficult to be detached from the biomass [64]. From Table 2, it is also noticed that desorption of MB dye was 6.5% in normal water and only 4% while highly concentrated acidic acid was used to reduce pH (=3.1) of aqueous solution. Therefore, the desorption study by strong inorganic nitric acid, organic acetic acid and normal water indicates that the adsorption phenomenon of MB dye onto EB material was mainly due to ion exchange along with strong physical and chemisorption in nature [65].

3.4. Adsorption kinetics and mechanism of adsorption

3.4.1. Application of pseudo-first-order model

In this section, the pseudo-first-order model was applied to investigate the adsorption nature of MB dye on EB biomass. Using Eq. (4), plots of log ($q_e - q_t$) vs. t for experimental data at various physico-chemical conditions are fitted for pseudo first order model which are not presented here where q_e and q_t refer to the amount of MB adsorbed (mg/g) at equilibrium and at time, t (min), respectively. From those plots, the pseudo-first-order rate constant (K_1) and linear regression coefficient (R^2) have been calculated which gives very poor value. Moreover, pseudo-first-order kinetic model predicts a much lower value of the equilibrium adsorption capacity than the experimental value, and hence, it gives the inapplicability of this model.

Table 2
Desorption of MB

pH	Initial MB concentration (mg/L)	Final MB concentration (mg/L)	Desorption (%)
2.5	8.440	3.898	46.18
3	5.700	2.066	36.25
3.5	4.660	1.290	27.68
4.1	3.850	0.661	17.17
5.5	2.880	0.287	9.97
8.7	2.630	0.220	8.37
Normal water	2.805	0.184	6.56
Acetic acid (conc. > 80%)	5.500	0.220	4.00

3.4.2. Application of pseudo-second-order model

To study the pseudo-second-order model, Eq. (5) is used to construct plots of t/q vs. t to fit experimental data at various physico-chemical conditions such as for initial dye concentration, initial solution pH, adsorbent dosages, temperature, ionic strength and for surfactant which plots are not presented here. The initial sorption rate h, pseudo-second-order rate constant K_2, amount of dye adsorbed at equilibrium q_e and the corresponding linear regression correlation coefficient R^2 values are determined from the slope and intercept of plot t/q_t vs. t which are tabulated in Table 3. The R^2 values were found to be close to 1. The higher R^2 values confirm that the sorption process follows pseudo-second-order mechanism. The experimental q_e values studied were close to calculated q_e values, indicating the strong correlation applicable for the pseudo-second-order model for MB dye adsorption kinetics on EB biomass. Therefore, it can be concluded that the kinetics of adsorption was followed by pseudo-second-order

Table 3
Pseudo-second-order model parameters for adsorption of MB dye on EB

System parameters	q_e (mg/g), experimental	K_2 (g/mg min)	q_e (mg/g), calculated	h (mg/g min)	R^2
Adsorbent dosage (mg)					
10	72.96	0.0012	73.53	6.75	0.9854
20	42.99	0.0062	42.92	11.39	0.9986
30	31.30	0.0082	30.86	7.79	0.9969
Initial metal ion concentration (ppm)					
20	42.99	0.0060	45.87	12.53	0.9992
30	61.14	0.0041	58.82	14.04	0.9980
40	61.10	0.0029	61.35	11.04	0.9980
50	61.32	0.0016	57.80	5.47	0.9931
60	67.91	0.0008	71.94	4.26	0.9931
70	71.98	0.0009	68.49	3.99	0.9574
pH					
2.5	28.90	0.0096	28.74	7.95	0.9981
3.5	38.35	0.0068	37.74	9.66	0.9977
5.25	42.81	0.0071	42.02	12.52	0.9982
7.4	42.99	0.0062	42.92	11.39	0.9986
8.3	43.43	0.0024	44.25	4.77	0.9885
10	44.73	0.0055	43.86	10.55	0.9964
Temperature (°C)					
30	42.99	0.0062	42.92	11.39	0.9986
45	44.46	0.0046	44.84	9.17	0.9976
60	45.39	0.0045	45.45	9.37	0.9975
Salt concentration (ppm)					
100 ppm NaCl	29.39	0.0007	32.68	0.78	0.8803
200 ppm NaCl	32.11	0.0002	45.05	0.44	0.5965
300 ppm NaCl	34.96	0.0006	32.36	0.66	0.7808
100 ppm $CaCl_2$	30.55	0.0023	31.45	2.28	0.9865
200 ppm $CaCl_2$	35.90	0.0011	39.22	1.62	0.9398
300 ppm $CaCl_2$	45.57	0.0158	45.87	33.22	0.9999
100 ppm $FeCl_3$	43.92	0.0010	46.51	2.14	0.9660
200 ppm $FeCl_3$	46.73	0.0010	49.75	2.54	0.9712
300 ppm $FeCl_3$	47.98	0.0015	51.02	4.01	0.9904
100 ppm (NaCl + $CaCl_2$)	54.69	0.0050	54.95	14.97	0.9986
Surfactant					
Triton X-100	38.80	0.0060	45.87	12.53	0.9992

reaction. The statement behind pseudo second order kinetic model indicates that the rate-limiting step might be chemisorption involving the valence forces through sharing or exchange of electrons between adsorbent and adsorbate [38,66]. Also from Table 3, it can be observed that the adsorption capacity increases with increase in initial dye concentration, initial solution pH, temperature and salt concentrations but decreases with amount of adsorbent, respectively. From Table 3, the values of rate constant, k_2, decrease with initial dye concentration for EB biomass. The reason for this behaviour may be due to the lower competition for the sorption sites at lower concentration. At higher concentrations, the competition for the surface active sites will be high, and consequently, lower sorption rates are obtained. The overall rate constant, k_2, increased as the adsorbent dosage increased, and also, initial adsorption rate, h, varied with the variation in the adsorbent dosage (Table 3). Similar types of kinetic model parameters were obtained by various researchers for a few other observation systems reported in the literature [8,16,20,49].

The half-adsorption time of the dye, $t_{1/2}$, that is the time required for EB to uptake half of the amount adsorbed at equilibrium, is often considered as a measure of the rate of adsorption and for the second-order process is given by the relationship [9].

$$t_{1/2} = 1/k_2 q_e \tag{14}$$

The calculated values of $t_{1/2}$ for the MB adsorption onto EB were 3.91, 4.03, 5.58, 9.97, 16.33 and 17.89 min for an initial concentration range of 20, 30, 40, 50, 60 and 70 ppm, respectively. Similarly for other process variables, $t_{1/2}$ have been calculated which are not presented here.

3.4.3. Application of intra-particle diffusion model and mechanism of MB adsorption

The mechanism of adsorption techniques involves four steps: migration of dye molecules from bulk solution to the surface of the sorbent, diffusion through the boundary layer to the surface of the sorbent, adsorption at a site and intra-particle diffusion into the interior of the sorbent [20].

The most commonly used technique for identifying the mechanism involved in the sorption process is by fitting the experimental data with intra-particle diffusion plot (Eq. 7). According to the intra-particle diffusion model, if a plot of the amount of sorbate adsorbed per unit weight of sorbent, q_t, vs. square root of contact time gives a linear plot, it indicates that intra-particle/pore diffusion is the rate-limiting step in the adsorption process [20]. The plot of amount sorbed per unit weight of sorbent, q_t (mg/g), vs. square root of time, $\sqrt{t}$, is shown in Fig. 12 for initial MB dye concentrations. Intra-particle diffusion plots for other kinetic parameters such as different solution pH, adsorbent dosages, different temperatures, ionic strength and surfactant are given same trend which are not presented here.

The plot obtained in Fig. 12 contrasts the prediction of the intra-particle diffusion model. It shows that the adsorption plot is not linear over the whole time range and can be separated into three linear regions which confirm the multi-stages of adsorption. The first part is attributed to boundary layer diffusion, the second to the intra-particle diffusion and the third to the chemical reaction [20]. Therefore, the presentation of the experimental data in Fig. 12 can be signified that the dye molecules were transported to the external surface of the EB particle through film diffusion and its rate was very fast. After that, MB dye molecules were entered into EB particles by intraparticle diffusion through pores. This indicates that the intra-particle diffusion is involved in the adsorption process of MB dye onto EB, but not the only rate-controlling step.

The diffusion coefficient, D_p, largely depends on the surface properties of adsorbents. The diffusion coefficient for the intra-particle transport of different initial concentrations of MB dye was also calculated using the following relationship [9]:

$$t_{0.5} = 0.03\ r_0^2/D_p \tag{15}$$

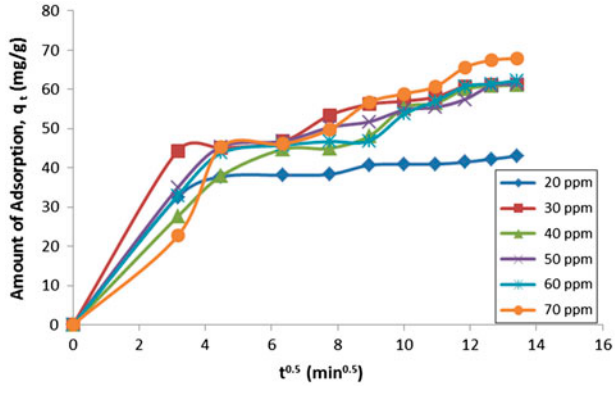

Fig. 12. Intra-particle diffusion model on different initial MB dye concentrations.

where $t_{1/2}$ is the half-life in seconds as calculated from Eq. (14). To calculate r_0, the radius of the adsorbent particle (cm), surface weighted mean diameter of EB particles of 25.26 μm (radius = 12.63 μm = 12.63 × 0.0001 cm = 0.001263 cm) has been utilized. The diffusion coefficient, D_p (cm^2/s), was calculated from Eq. (13), and the values were found to be 1.23×10^{-8} cm^2/s, 1.19×10^{-8} cm^2/s, 8.57×10^{-9} cm^2/s, 4.80×10^{-9} cm^2/s, 2.93×10^{-9} cm^2/s and 2.68×10^{-9} cm^2/s for an initial MB concentration of 20, 30, 40, 50, 60 and 70 ppm, respectively. The D_p values for MB on EB are much lower than those of benzene derivatives. The D_p values of phenol and benzene on carbon are 901×10^{-10} and 80×10^{-10} cm^2/s, respectively [9]. This was attributed to the larger molecular size of the present systems, the factor that slows down in diffusion rate [67]. In addition due to strong interaction between MB and EB, mobility was low [9].

3.4.4. Validity of various kinetic models

The adsorption kinetics of MB dye onto EB was further verified at different initial concentrations. The validity of each model was also determined by the sum of squared errors (SSE, %) calculated as given by:

$$\text{SSE, } \% = \sqrt{\frac{\sum (q_{e,exp} - q_{e,cal})^2}{N}} \quad (16)$$

where N is the number of data points.

The lower the value of SSE indicates, the better a fit is. It was found that the pseudo-second order kinetic model yielded the lowest SSE value of 3.01% compared to 56.34% for the pseudo-first-order kinetic model and 46.80% for the intra-particle diffusion model. This is also agreement with the R^2 values obtained and proves that the adsorption of MB dye onto the EB biomass could be best described by the pseudo-second-order kinetic model.

3.5. Adsorption equilibrium isotherm

Analysis of adsorption isotherm is of fundamental importance to describe how adsorbate molecules interact with the adsorbent surface. Equilibrium studies determine the capacity of the adsorbent and describe the adsorption mechanism. The experimental data were fitted to the Freundlich and Langmuir isotherm equations, and isotherm parameters were calculated. Linear regression analysis was then used to determine the best fitted isotherm.

3.5.1. Freundlich adsorption isotherm

Freundlich model is developed to explain how adsorption takes place on heterogeneous surfaces [68]. To study the Freundlich isotherm, adsorption equilibrium data were fitted with experimental data which is presented in Fig. 13. The value of correlation coefficient, R^2, of the Freundlich isotherm fit is 0.8973. K_f and n are the Freundlich constants with n giving an indication of how favourable the adsorption process is. The values of K_f and n are calculated from the slope and intercept of the plot (Fig. 13) where $\ln q_e$ vs. $\ln C_e$ using Eq. (8). The value of slope $1/n$ is 0.2966 ranging between 0 and 1 is a measure of adsorption intensity or surface heterogeneity becoming more heterogeneous as its value gets closer to zero [66]. All the parameters are depicted in Table 4. The value of n is larger than 1, indicating the favourable nature of adsorption [69].

3.5.2. Langmuir adsorption isotherm

The study of the Langmuir isotherm is essential in assessing the adsorption efficiency of the adsorbent. The Langmuir isotherm model is valid for monolayer adsorption onto a surface containing finite number of identical sites of uniform strategies of adsorption with no transmigration of adsorbate in the plane of surface [70]. This study is also useful in optimizing the operating conditions for effective adsorption. Langmuir isotherms (Eqs. 9 and 10) are found to be obeyed by MB dye on EB biomass as shown in Fig. 14(a) and (b). This indicates that the dyes are chemisorbed on the surface of EB. These logarithmic equations for the adsorption studies of MB dye on EB gave high linearity with a range of correlation coefficient between

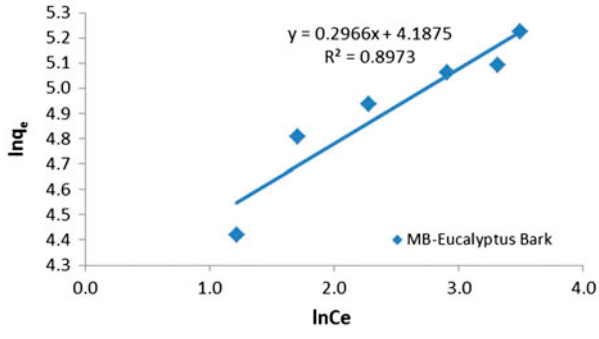

Fig. 13. Freundlich plot: amount of adsorbent 10 mg; initial MB concentration = 20, 30, 40, 50, 60 and 70 ppm, solution pH 9.9 ≈ 10.2, temperature = 30°C; shaker speed = 120 rpm; and time of adsorption = 180 min.

Table 4
A summary of Freundlich and Langmuir calculated values

Freundlich		
K_f (mg/g)	$1/n$ (L/g)	R^2
65.86	0.2966	0.8973
Langmuir (Type I)		
q_m (mg/g)	K_a (L/g)	R^2
204.08	0.2178	0.9588
Langmuir (Type Ii)		
q_m (mg/g)	K_a (L/g)	R^2
200.00	0.2262	0.9882

0.9588 and 0.9822. The Langmuir isotherm fits the experimental data very well. The maximum adsorption capacity, q_m (mg/g), and K_L values for Langmuir constants can be obtained from the linear equations of different plots (Fig. 14(a) and (b)).

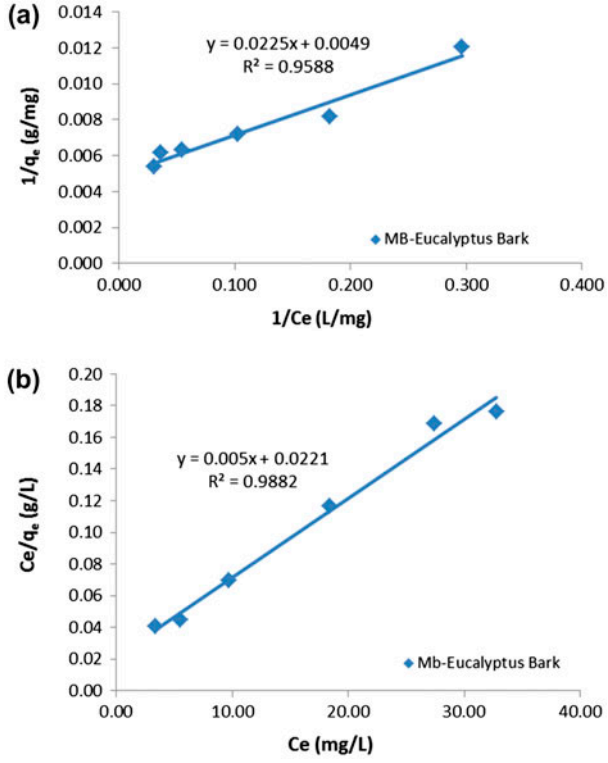

Fig. 14. (a) Equilibrium adsorption isotherm fitted to the Langmuir II model: amount of adsorbent added = 10 mg; initial MB dye concentration = 20, 30, 40, 50, 60, 70 ppm; solution pH 9.9 ≈ 10.2; temperature = 30˚C; shaker speed = 120 rpm; and time of adsorption = 180 min. (b) Equilibrium adsorption isotherm fitted to the Langmuir I model: amount of adsorbent added = 10 mg; initial MB dye concentration = 20, 30, 40, 50, 60, 70 ppm; solution pH 9.9 ≈ 10.2; temperature = 30˚C; shaker speed = 120 rpm; and time of adsorption = 180 min.

The linear regression coefficient (R^2) for the two types of Langmuir model presents high values compared to Freundlich model which gives a clear indication that Langmuir model is best fitted with the equilibrium data. The values of Freundlich and Langmuir model parameters are summarized and presented in Table 4.

The separation factor (R_L) is a dimensionless constant which is used to investigate the adsorption system feasibility at different initial dye concentration and can be determined from Langmuir plot as per the following relation:

$$R_L = \frac{1}{1 + K_a C_0} \tag{17}$$

The R_L values, using Eq. (17), for the adsorption of MB onto EB are in the range of 0.06–0.19. The R_L values obtained are found to decrease with the increment of initial MB solution concentration and as $0 < R_L < 1$, this indicated that the adsorption of MB onto EB is a favourable adsorption process [39].

The maximum adsorption value, q_m (mg/g), obtained in the present study was compared with those of other sorbents for MB adsorption from other studies which are presented in Table 5. From Table 5, it can be found that raw EB is very good effective adsorbent for the removal of MB dye from its aqueous solution and it is better than many agricultural by-products and activated carbons.

3.6. Thermodynamic studies

To understand the changes in the reaction that can be expected during the process, the thermodynamics parameters have been calculated. The linear form of the plot log (q_e/C_e) vs. $1/T$ has been used to calculate the thermodynamics parameters utilizing Eq. (12) along with Eq. (13). Various thermodynamic parameters are presented in Table 6. From Table 6, the change in Gibbs free energy (ΔG°) was found to be negative at all temperatures, while enthalpy (ΔH°) was positive, suggesting endothermic and irreversible nature of the process. The negative value of ΔG° confirmed the feasibility of the process and the spontaneous nature of sorption with a high preference of MB dye on EB. The ΔG° value becomes more negative with increasing temperature supports that MB adsorption on EB is favoured with the increase in temperature. The positive value of entropy (ΔS°) indicates favourable randomness factor though its value is small. This

Table 5
Comparison of the adsorption capacity (q_m in mg/g) of different sorbents for the removal of MB dye

Adsorbent	Maximum adsorption capacity, q_m (mg/g)	Reference
Wood apple shell	95.2	[18]
Pine cone biomass	109.89	[9]
Zeolite	25	[71]
Powdered activated carbon	91	[72]
Granular activated carbon	21.5	[72]
Orange peels	18.60	[19]
Raw date pits	80.30	[73]
Neem leaf	19.61	[74]
Cotton waste	24.00	[75]
Wheat bran carbon (25°C)	122.0	[76]
Ground palm kernel coat	277.22	[77]
Gulmohar plant leaf powder	186.22	[46]
Wood	84	[75]
Coconut husk	99	[20]
Fly ash	1.3	[78]
Banana peel	20.8	[19]
Clay	58.2	[79]
Rice husk	40.59	[8]
Caster seed shell	158.73	[20]
Eucalyptus bark	204.08	Present study

Table 6
Thermodynamic parameters for adsorption of MB dye at different temperature

Temp. (K)	ΔG° (kJ/mole)	ΔH° (kJ/mole)	ΔS° (kJ/mole K)
303.15	−6.89		
318.15	−7.89	13.3089	0.0666
333.15	−8.89		

suggests the structural changes after adsorption of MB dye takes place on bark [29].

4. Design of single-stage batch adsorber from isotherm data

The design of a single-stage batch adsorption system was determined from the Langmuir adsorption isotherm data using the method developed by Vadivelan and Kumar [8]. Due to lack of extensive experimental data, empirical design procedures based on adsorption isotherm studies are the most common method to predict the adsorber size and performance [31]. The design objective was to reduce initial MB dye concentration of C_0 (ppm) to C_t (ppm) for which total dye solution is V (L). The amount of added adsorbent was m (g), and the solute loading changes from q_0 (mg/g) to q_t (mg/g) where $q_0 = 0$. The mass balance for MB dye in the single-stage operation under equilibrium is expressed as [31]:

$$V(C_0 - C_e) = m(q_e - q_0) = mq_e \tag{18}$$

Eq. (17) can be written by rearranging Eqs. (7) and (16) after putting the value of q_e as

$$\frac{m}{V} = \frac{C_0 - C_e}{q_e} = \frac{C_0 - C_e}{\frac{q_m K_a C_e}{1 + K_a C_e}} \tag{19}$$

Fig. 15 shows a series of plots derived from Eq. (18) where the predicted amount of EB particles required to remove dye solutions of initial concentrations of 100 ppm for 90, 80, 70 and 60% colour removal at different solution volumes (1–10 L). This is an outline of design procedure for a single-stage batch

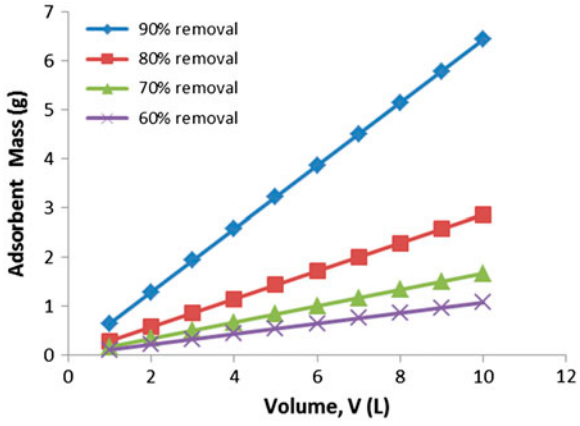

Fig. 15. Adsorbent mass (m) against volume of solution treated (L).

adsorption system presented by Vadivelan and Kumar [8].

5. Conclusion

In this study, raw EB was utilized as a low-cost adsorbent for MB removal from aqueous solution. The main conclusions which can be drawn on the basis of this study are as follows:

(1) The adsorption equilibrium was reached within 140 min. Kinetic experiments clearly indicated that adsorption of MB dye on EB biomass is a multi-step process: a rapid adsorption of dye onto the external surface followed by intra-particle diffusion into the interior of adsorbent which has also been confirmed by intra-particle diffusion model. Overall, the kinetic studies showed that the MB dye adsorption process followed pseudo-second-order kinetic model and the adsorption was controlled by chemisorption process.

(2) The amount of MB dye adsorption on EB was found to increase with an increase in initial solution pH, initial MB dye concentration, contact time, ionic strength and system temperature; but decreased with increase in the amount of adsorbent and non-ionic surfactant.

(3) EB biomass has a good adsorption capacity to adsorb both cationic dye MB and anionic dye CR.

(4) The presence of monovalent salt in the MB dye solution reduced the percentage removal of MB dye, whereas divalent and trivalent salts in the MB dye solution enhanced the removal efficiency of EB biomass, and by increasing the salt concentrations, the biosorption capacity of EB further increased.

(5) The experimental data correlated reasonably well by both Langmuir I and Langmuir II adsorption isotherms where adsorption capacity was found to be 204.08 mg/g. The dimensionless separation factor (R_L) showed that the EB biomass could be used for the removal of MB from aqueous solution.

(6) Desorption experiments clearly indicated that adsorption of MB dye followed ion exchange and strong physical chemical adsorption.

(7) Finally, thermodynamic parameters were determined at three different temperatures. From the results of positive enthalpy change (ΔH°) accompanied by positive entropy change (ΔS°) and negative decrease in Gibbs free energy change (ΔG°), it is evident that the adsorption process is endothermic, irreversible and spontaneous in nature.

This study demonstrates that EB, an agro-based waste and inexpensive biomaterial, can be an alternative for many expensive adsorbents used for the removal of MB dye in wastewater treatment.

Symbols

C_e — equilibrium dye concentration, ppm
C_0 — initial dye concentration, ppm
C_t — dye concentration at time t, ppm
D_p — diffusion coefficient, cm^2/s
ΔG° — Gibbs free energy change, kJ/mol
ΔH° — enthalpy change, kJ/mol
h — initial adsorption rate, mg/g min
Ka — langmuir constant
K_1 — pseudo-first-order rate constant, min^{-1}
K_2 — pseudo-second-order rate constant, mg/g min
K_f — Freundlich adsorption constant, mg/g
K_{id} — intra-particle rate constant, mg/g $min^{0.5}$
M — mass of adsorbent per unit volume, g L^{-1}
m — amount of adsorbent added, g
n — Freundlich constant
q — amount of adsorbate per g of adsorbent, mg/g
q_e — amount of adsorbate per g of adsorbent at equilibrium, mg/g
q_t — amount of adsorbate per g of adsorbent at any time, t
q_m — equilibrium adsorption capacity using model
q_{max} — maximum adsorption capacity, mg/g
R_2 — linear regression coefficient
R_L — separation factor
r_0 — radius of adsorbent particle, cm
ΔS° — entropy change, J/k mol
t — time, min
T — temperature, K

References

[1] K. Ravikumar, B. Deebika, K. Balu, Decolourization of aqueous dye solutions by a novel adsorbent: Application of statistical designs and surface plots for the optimization and regression analysis, J. Hazard. Mater. 122 (2005) 75–83.

[2] T. Padmesh, K. Vijayaraghavan, G. Sekaran, M. Velan, Biosorption of Acid Blue 15 using fresh water macroalga *Azolla filiculoides*: Batch and column studies, Dyes Pigm. 71 (2006) 77–82.

[3] C. O'Neill, F.R. Hawkes, D.L. Hawkes, N.D. Lourenço, H.M. Pinheiro, W. Delée, Colour in textile effluents–sources, measurement, discharge consents and simulation: A review, J. Chem. Technol. Biotechnol. 74 (1999) 1009–1018.

[4] P.C. Vandevivere, R. Bianchi, W. Verstraete, Review: Treatment and reuse of wastewater from the textile wet-processing industry: Review of emerging technologies, J. Chem. Technol. Biotechnol. 72 (1998) 289–302.

[5] G.E. Walsh, L.H. Bahner, W.B. Horning, Toxicity of textile mill effluents to freshwater and estuarine algae, crustaceans and fishes, Environ. Pollut. Ser. A, Ecol. Biol. 21 (1980) 169–179.

[6] A. Milani, A. Ciammella, C. Degen, M. Siciliano, L. Rossi, Ascites dynamics in cirrhosis, J. Hepatol. 16 (1992) 369–375.

[7] N. Bélaz-David, L. Decosterd, M. Appenzeller, Y. Ruetsch, R. Chioléro, T. Buclin, J. Biollaz, Spectrophotometric determination of methylene blue in biological fluids after ion-pair extraction and evidence of its adsorption on plastic polymers, Eur. J. Pharm. Sci. 5 (1997) 335–345.

[8] V. Vadivelan, K.V. Kumar, Equilibrium, kinetics, mechanism, and process design for the sorption of methylene blue onto rice husk, J. Colloid Interface Sci. 286 (2005) 90–100.

[9] T.K. Sen, S. Afroze, H. Ang, Equilibrium, kinetics and mechanism of removal of methylene blue from aqueous solution by adsorption onto pine cone biomass of *Pinus radiata*, Water Air Soil Pollut. 218 (2011) 499–515.

[10] A. Bhatnagar, A. Minocha, Conventional and nonconventional adsorbents for removal of pollutants from water—A review, Indian J. Chem. Technol. 13 (2006) 203–217.

[11] L.M. Cotoruelo, M.D. Marqués, F.J. Díaz, J. Rodríguez-Mirasol, J.J. Rodríguez, T. Cordero, Equilibrium and kinetic study of Congo red adsorption onto lignin-based activated carbons, Transp. Porous Media. 83 (2010) 573–590.

[12] M.T. Yagub, T.K. Sen, M. Ang, Removal of cationic dye methylene blue (MB) from aqueous solution by ground raw and base modified pine cone powder, Environ. Earth Sci. 71 (2014) 1507–1519.

[13] M.A.M. Salleh, D.K. Mahmoud, W.A.W.A. Karim, A. Idris, Cationic and anionic dye adsorption by agricultural solid wastes: A comprehensive review, Desalination 280 (2011) 1–13.

[14] M. Rafatullah, O. Sulaiman, R. Hashim, A. Ahmad, Adsorption of methylene blue on low-cost adsorbents: A review, J. Hazard. Mater. 177 (2010) 70–80.

[15] A. Mittal, J. Mittal, A. Malviya, V. Gupta, Removal and recovery of Chrysoidine Y from aqueous solutions by waste materials, J. Colloid Interface Sci. 344 (2010) 497–507.

[16] P. Senthil Kumar, S. Ramalingam, C. Senthamarai, M. Niranjanaa, P. Vijayalakshmi, S. Sivanesan, Adsorption of dye from aqueous solution by cashew nut shell: Studies on equilibrium isotherm, kinetics and thermodynamics of interactions, Desalination 261 (2010) 52–60.

[17] M.T. Yagub, T.K. Sen, H. Ang, Equilibrium, kinetics, and thermodynamics of Methylene Blue adsorption by pine tree leaves, Water Air Soil Pollut. 223 (2012) 5267–5282.

[18] S. Jain, R.V. Jayaram, Removal of basic dyes from aqueous solution by low-cost adsorbent: Wood apple shell (*Feronia acidissima*), Desalination 250 (2010) 921–927.

[19] G. Annadurai, R.-S. Juang, D.-J. Lee, Use of cellulose-based wastes for adsorption of dyes from aqueous solutions, J. Hazard. Mater. 92 (2002) 263–274.

[20] N. Oladoja, C. Aboluwoye, Y. Oladimeji, A. Ashogbon, I. Otemuyiwa, Studies on castor seed shell as a sorbent in basic dye contaminated wastewater remediation, Desalination 227 (2008) 190–203.

[21] M.T. Yagub, T.K. Sen, S. Afroze, H. Ang, Dye and its removal from aqueous solution by adsorption: A review, Adv. Colloid Interface Sci. 209 (2014) 172–184.

[22] H. Ali, Biodegradation of synthetic dyes—A review, Water Air Soil Pollut. 213 (2010) 251–273.

[23] S. Sadaf, H.N. Bhatti, Batch and fixed bed column studies for the removal of Indosol Yellow BG dye by peanut husk, J. Taiwan Inst. Chem. Eng. 45 (2014) 541–553.

[24] L. Morais, O. Freitas, E. Gonçalves, L. Vasconcelos, C. González Beça, Reactive dyes removal from wastewaters by adsorption on eucalyptus bark: Variables that define the process, Water Res. 33 (1999) 979–988.

[25] I. Ghodbane, L. Nouri, O. Hamdaoui, M. Chiha, Kinetic and equilibrium study for the sorption of cadmium(II) ions from aqueous phase by eucalyptus bark, J. Hazard. Mater. 152 (2008) 148–158.

[26] V. Sarin, K.K. Pant, Removal of chromium from industrial waste by using eucalyptus bark, Bioresour. Technol. 97 (2006) 15–20.

[27] R. Saliba, H. Gauthier, R. Gauthier, M. Petit-Ramel, The use of eucalyptus barks for the adsorption of heavy metal ions and dyes, Adsorpt. Sci. Technol. 20 (2002) 119–129.

[28] I. Ghodbane, O. Hamdaoui, Removal of mercury(II) from aqueous media using eucalyptus bark: Kinetic and equilibrium studies, J. Hazard. Mater. 160 (2008) 301–309.

[29] P.N. Dave, S. Kaur, E. Khosla, Removal of Eriochrome black-T by adsorption on to eucalyptus bark using green technology, Indian J. Chem. Technol. 18 (2011) 53–60.

[30] R. Srivastava, D. Rupainwar, Eucalyptus bark powder as an effective adsorbent: Evaluation of adsorptive characteristics for various dyes, Desalin. Water Treat. 11 (2009) 302–313.

[31] S. Dawood, T.K. Sen, C. Phan, Synthesis and characterisation of novel-activated carbon from waste biomass pine cone and its application in the removal of congo red dye from aqueous solution by adsorption, Water Air Soil Pollut. 225 (2014) 1–16.

[32] S. Lagergren, Zur theoric der sogenannten adsorption geloster stoffe (About the theory of so-called adsorption of soluble substances), Kungliga Svenska Vetenskapsakademiens Handlingar 24(4) (1898) 1–39.
[33] B. Nandi, A. Goswami, M. Purkait, Removal of cationic dyes from aqueous solutions by kaolin: Kinetic and equilibrium studies, Appl. Clay Sci. 42 (2009) 583–590.
[34] T.K. Sen, M.V. Sarzali, Removal of cadmium metal ion (Cd^{2+}) from its aqueous solution by aluminium oxide (Al_2O_3): A kinetic and equilibrium study, Chem. Eng. J. 142 (2008) 256–262.
[35] H. Freundlich, Over the adsorption in solution, J. Phys. Chem. 57 (1906) 385–470.
[36] I. Langmuir, The adsorption of gases on plane surfaces of glass, mica and platinum, J. Am. Chem. Soc. 40 (1918) 1361–1403.
[37] A. Pérez-Marín, V.M. Zapata, J. Ortuño, M. Aguilar, J. Sáez, M. Lloréns, Removal of cadmium from aqueous solutions by adsorption onto orange waste, J. Hazard. Mater. 139 (2007) 122–131.
[38] F. Arias, T.K. Sen, Removal of zinc metal ion (Zn^{2+}) from its aqueous solution by kaolin clay mineral: A kinetic and equilibrium study, Colloids Surf., A 348 (2009) 100–108.
[39] P. Baskaralingam, M. Pulikesi, D. Elango, V. Ramamurthi, S. Sivanesan, Adsorption of acid dye onto organobentonite, J. Hazard. Mater. 128 (2006) 138–144.
[40] University of Colorado, Table of Characteristic IR Absorptions, 1985. Available from: http://orgchem.colorado.edu/Spectroscopy/specttutor/irchart.pdf.
[41] Wellesley College, Table 1: Principal IR Absorptions for Certain Functional Groups, 1875. Available from: http://academics.wellesley.edu/Chemistry/chem211lab/Orgo_Lab_Manual/Appendix/Instruments/InfraredSpec/Chem211%20IR%20Lit%20Value%20Table.pdf.
[42] B.C. Lippens, J. De Boer, Studies on pore systems in catalysts V. The t method. J. Catal. 4 (1965) 319–323.
[43] A. Jumasiah, T.G. Chuah, J. Gimbon, T.S.Y. Choong, I. Azni, Adsorption of basic dye onto palm kernel shell activated carbon: Sorption equilibrium and kinetics studies, Desalination 186 (2005) 57–64.
[44] Y. Bulut, H. Aydın, A kinetics and thermodynamics study of methylene blue adsorption on wheat shells, Desalination 194 (2006) 259–267.
[45] V. Ponnusami, S. Vikram, S. Srivastava, Guava (*Psidium guajava*) leaf powder: Novel adsorbent for removal of methylene blue from aqueous solutions, J. Hazard. Mater. 152 (2008) 276–286.
[46] V. Ponnusami, V. Gunasekar, S. Srivastava, Kinetics of methylene blue removal from aqueous solution using gulmohar (*Delonix regia*) plant leaf powder: Multivariate regression analysis, J. Hazard. Mater. 169 (2009) 119–127.
[47] P.S. Kumar, S. Ramalingam, K. Sathishkumar, Removal of methylene blue dye from aqueous solution by activated carbon prepared from cashew nut shell as a new low-cost adsorbent, Korean J. Chem. Eng. 28 (2011) 149–155.
[48] Z. Shahryari, A.S. Goharrizi, M. Azadi, Experimental study of methylene blue adsorption from aqueous solutions onto carbon nano tubes, Int. J. Water Resour. Environ. Eng. 2 (2010) 16–28.
[49] M.A. El-Latif, A.M. Ibrahim, M. El-Kady, Adsorption equilibrium, kinetics and thermodynamics of methylene blue from aqueous solutions using biopolymer oak sawdust composite, J. Am. Sci. 6 (2010) 267–283.
[50] S. Arivoli, M. Hema, S. Parthasarathy, N. Manju, Adsorption dynamics of methylene blue by acid activated carbon, J. Chem. Pharm. Res. 2 (2010) 626–641.
[51] M.A. Rahman, S.R. Amin, A.S. Alam, Removal of Methylene Blue from waste water using activated carbon prepared from rice husk, Dhaka Univ. J. Sci. 60 (2012) 185–189.
[52] Z. Al-Qodah, Adsorption of dyes using shale oil ash, Water Res. 34 (2000) 4295–4303.
[53] T. Tarawou, M. Horsfall Jr., Adsorption of methylene blue dye on pure and carbonized water weeds, Biorem. J. 11 (2007) 77–84.
[54] E.O. Oyelude, F. Appiah-Takyi, Removal of methylene blue from aqueous solution using alkali-modified malted sorghum mash, Turkish J. Eng. Environ. Sci. 36 (2012) 161–169.
[55] M. Doğan, H. Abak, M. Alkan, Biosorption of methylene blue from aqueous solutions by hazelnut shells: Equilibrium, parameters and isotherms, Water Air Soil Pollut. 192 (2008) 141–153.
[56] K. Bharathi, S. Ramesh, Removal of dyes using agricultural waste as low-cost adsorbents: A review, Appl. Water Sci. 3 (2013) 773–790.
[57] C.-Y. Kuo, C.-H. Wu, J.-Y. Wu, Adsorption of direct dyes from aqueous solutions by carbon nanotubes: Determination of equilibrium, kinetics and thermodynamics parameters, J. Colloid Interface Sci. 327 (2008) 308–315.
[58] M. Fedoseeva, P. Fita, A. Punzi, E. Vauthey, Salt effect on the formation of dye aggregates at liquid/liquid interfaces studied by time-resolved surface second harmonic generation, J. Phys. Chem. C 114 (2010) 13774–13781.
[59] X.S. Wang, Y. Zhou, Y. Jiang, C. Sun, The removal of basic dyes from aqueous solutions using agricultural by-products, J. Hazard. Mater. 157 (2008) 374–385.
[60] S. Zaheer, H.N. Bhatti, S. Sadaf, Y. Safa, M. Zia-ur-Rehman, Biosorption characteristics pf sigarcanr bagasse for the removal of foron blue e-el dye from aqueous solutions, J. Anim. Plant Sci. 24 (2014) 272–279.
[61] I.u. Haq, H.N. Bhatti, M. Asgher, Removal of solar red BA textile dye from aqueous solution by low cost barley husk: Equilibrium, kinetic and thermodynamic study, Can. J. Chem. Eng. 89 (2011) 593–600.
[62] Ü. Geçgel, G. Özcan, G.Ç. Gürpınar, Removal of methylene blue from aqueous solution by activated carbon prepared from pea shells (*Pisum sativum*), J. Chem. 2013 (2012) 9. Available from: http://dx.doi.org/10.1155/2013/614083.
[63] L.K. Brahimi-Horn MC, S.L. Liany, D.G. Mou, Binding of textile azo dyes by *Morothecium verrucaria* Orange II, 10B (blue) and RS (red) azo dye uptake for textile wastewater decolourization, J. Microbiol. 10 (1992) 245–261.
[64] M. Horsfall Jr., F.E. Ogban, E.E. Akporhonor, Recovery of lead and cadmium ions from metal-loaded biomass of wild cocoyam (Caladium bicolor) using acidic, basic and neutral eluent solutions, Electron. J. Biotechnol. 9 (2006) 152–156.
[65] S. Ramalakshmi, K. Muthuchelian, K. Swaminathan, Kinetic and equilibrium studies on biosorption of reactive blacks dye from aqueous solution by native and treated fungi *Alternaria raphani*, J. Biosci. Res. 2 (2011) 239–248.

[66] F. Haghseresht, G. Lu, Adsorption characteristics of phenolic compounds onto coal-reject-derived adsorbents, Energy Fuels 12 (1998) 1100–1107.
[67] S. Dawood, T.K. Sen, Removal of anionic dye Congo red from aqueous solution by raw pine and acid-treated pine cone powder as adsorbent: Equilibrium, thermodynamic, kinetics, mechanism and process design, Water Res. 46 (2012) 1933–1946.
[68] I. Tan, A. Ahmad, B. Hameed, Adsorption of basic dye using activated carbon prepared from oil palm shell: Batch and fixed bed studies, Desalination 225 (2008) 13–28.
[69] H. Demiral, İ. Demiral, F. Tümsek, B. Karabacakoğlu, Adsorption of chromium(VI) from aqueous solution by activated carbon derived from olive bagasse and applicability of different adsorption models, Chem. Eng. J. 144 (2008) 188–196.
[70] I. Langmuir, The constitution and fundamental properties of solids and liquids. Part I. Solids, J. Am. Chem. Soc. 38 (1916) 2221–2295.
[71] L. Markovska, V. Meško, V. Noveski, M. Marinkovski, Solid diffusion control of the adsorption of basic dyes onto granular activated carbon and natural zeolite in fixed bed columns, J. Serb. Chem. Soc. 66 (2001) 463–475.
[72] J. Yener, T. Kopac, G. Dogu, T. Dogu, Dynamic analysis of sorption of methylene blue dye on granular and powdered activated carbon, Chem. Eng. J. 144 (2008) 400–406.
[73] T. Robinson, G. McMullan, R. Marchant, P. Nigam, Remediation of dyes in textile effluent: A critical review on current treatment technologies with a proposed alternative, Bioresour. Technol. 77 (2001) 247–255.
[74] K.G. Bhattacharyya, A. Sharma, Kinetics and thermodynamics of Methylene Blue adsorption on Neem (*Azadirachta indica*) leaf powder, Dyes Pigm. 65 (2005) 51–59.
[75] G. McKay, V.J. Poots, Kinetics and diffusion processes in colour removal from effluent using wood as an adsorbent, J. Chem. Technol. Biotechnol. 30 (1986) 279–282.
[76] A. Özer, G. Dursun, Removal of methylene blue from aqueous solution by dehydrated wheat bran carbon, J. Hazard. Mater. 146 (2007) 262–269.
[77] N. Oladoja, C. Aboluwoye, Y. Oladimeji, Kinetics and isotherm studies on Methylene Blue adsorption onto ground palm kernel coat, Turkish J. Eng. Environ. Sci. 32 (2008) 303–312.
[78] C. Woolard, J. Strong, C. Erasmus, Evaluation of the use of modified coal ash as a potential sorbent for organic waste streams, Appl. Geochem. 17 (2002) 1159–1164.
[79] A. Gurses, C Dogar, M. Yalcin, M. Acikyildiz, R. Bayrak, S. Karaca, The adsorption kinetics of the cationic dye, methylene blue, onto clay, J. Hazard. Mater. 131 (2006) 217–228.